

Modelling Materials Properties Critical to Simulation of Hot Stamping

Z. Guo¹⁾, G. Kang²⁾, N. Saunders¹⁾

¹⁾ Sente Software Ltd., Surrey Technology Centre, Guildford / U.K. ²⁾ Marketing Lab, Seo-Gu, Daejeon / Korea

Reliable simulation of hot stamping process requires accurate material data. This paper describes the development of computer models that can provide many of the material data required, including TTT/CCT phase transformation diagrams, temperature dependent physical and thermophysical properties, as well as temperature and strain rate dependent mechanical properties including high temperature strength and flow stress curves. The calculated material data have been used to simulate the hot stamping production of a part made of steel 22MnB5. The simulation is carried out with coupled analysis of heat transfer, deformation mechanics and phase transformations. The simulated springback is in good agreement with the experimental observation.

Keywords: Hot stamping, Processing simulation, Material properties, TTT/CCT diagrams, High strength steels.

Introduction

Hot stamping (HS) is an advanced manufacturing process in which a high strength part is produced by forging at high temperatures, followed by rapid-cooling in the forging dies [1,2]. Combining forming and hardening in one operation, results in extensive cost savings and good crash performance. As the material has excellent formability at high temperatures, complex shapes can be formed in a single stroke. Also, because the part remains in the die during the cooling stage, springback is minimized [2].

To achieve reliable computer-aided engineering (CAE) simulation of the HS process, or any thermo-mechanical processing in general, high quality material data input is required. For example, physical and mechanical properties as well phase transformation kinetics are needed for the simulation of a practical processing operation. The traditional way of obtaining material data is through experimentation, which is both expensive and time-consuming. Lack of material data has been a common problem in CAE simulation, even though there are many software packages available. To overcome this problem and provide reliable and cost effective data for process simulation, computer-based models have been developed so that such properties can be readily calculated [3].

The paper consists of two parts. The first part gives a brief description of the calculations that have been made to obtain the requisite materials properties for HS processing. The second part features the simulation of a V-bending process itself. The simulation is carried out with coupled analysis of heat transfer, deformation mechanics, and phase transformations.

Modelling of Materials Properties Using JMatPro

The hot stamping operation investigated in this work is a V-bending process. The process consists of five steps: heating in furnace, transportation to the press stage, hot forming, quenching, and unloading. **Figure 1** shows the three main processing steps. Any simulation must be able to deal with heat transfer, phase transformation and material deformation, in a coupled fashion.

Simulation of heat transfer requires knowledge of thermal conductivity and heat capacity. Simulation of deformation requires elastic modulus, Poisson's ratio, thermal expansion coefficient, strength and flow stress curves. All of these properties are required as a function of temperature and/or strain rate. Phase transformation simulation requires the knowledge of transformation kinetics, as well as heat evolution and volume change during transformations.

The material of interest is a 22MnB5 alloy, with composition (wt.%): Fe-0.24C-0.17Cr-1.14Mn-0.27Si-0.036Ti-0.003B-0.015P-0.001S. The materials properties required for hot stamping simulation are calculated by the computer software JMatPro [3,4,5]. The material models employed by JMatPro are briefly introduced below, followed by examples of calculated properties for the 22MnB5 alloy.

TTT/CCT Diagrams. The material models employed in JMatPro are able to calculate TTT/CCT diagrams for steels over a wide composition range [6,7]. The composition of the austenite at the quenching temperature is always used in the calculation. The TTT curves of the 22MnB5 alloy are given in **Figure 2**, where the austenite grain size is taken as 33 μm .

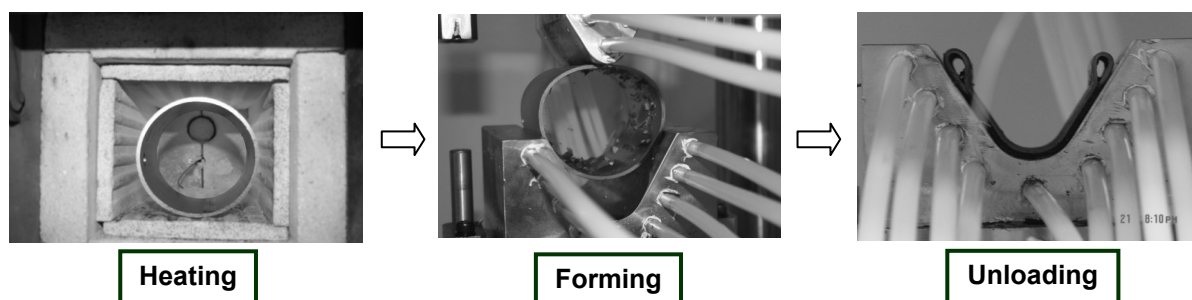


Figure 1. V-Bending experiment at elevated temperature.

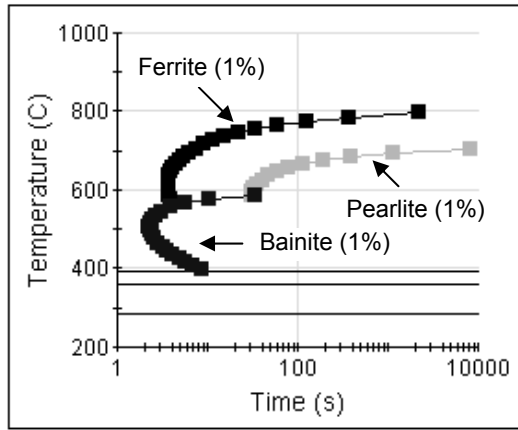


Figure 2. TTT curves of 22MnB5 calculated by JMatPro.

The formation of martensite and bainite is affected by the prior formation of ferrite. The carbon rejected by the formation of ferrite is incorporated into the remaining

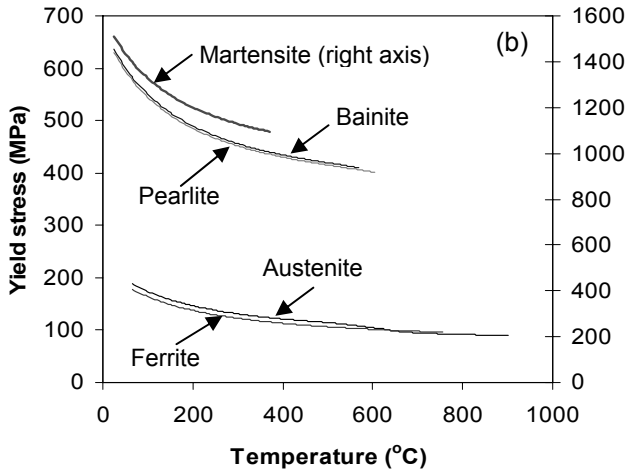
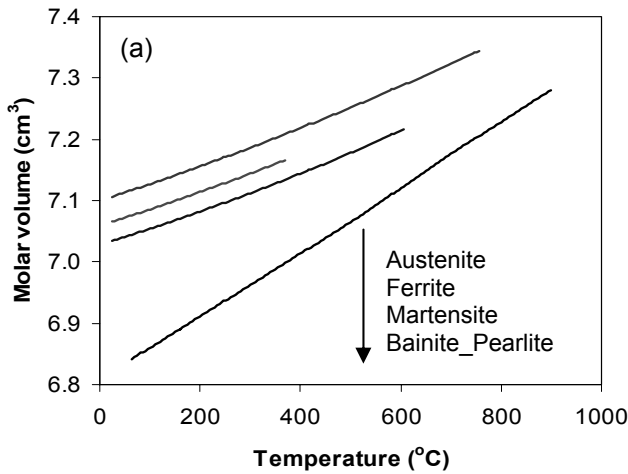


Figure 3. Molar volume and proof stress of various phases during cooling at 10°C/s.

austenite, which may significantly affect further transformations. For example, increased carbon in austenite reduces bainite start (Bs) and martensite start (Ms) temperatures, and increases the strength of the transformed phases. The Ms temperature is about 370 and 390°C for cooling at 10 and 50°C/s, respectively. A cooling rate of 50°C/s results in a complete transformation to martensite.

Physical and Thermophysical Properties. JMatPro's ability to calculate physical and thermophysical properties has been well documented in previous work for various metallic systems [3,5,6,8]. Such properties include, for example, density, molar volume, thermal expansion coefficient, thermal conductivity, Young's modulus, Poisson's ratio and specific heat. Such materials properties can be provided for each phase if required. Figure 3(a) uses molar volume as an example to demonstrate this capability.

Mechanical Properties – Strength and Flow Stress Curve. The calculation of strength and hardness of an alloy during cooling has been described previously in Ref. [9]. JMatPro is capable of providing either the overall strength/hardness or that for each phase. Figure 3(b) is the calculated $\sigma_{0.2}$ proof stress for each phase during cooling at 10°C/s. One usually expects the pearlite to be weaker in comparison with bainite. However, this may not

always be the case, as is demonstrated by the hardness and phases present in a 20MnCr5 as a function of cooling rate [10]. In this case, there is only a small change in hardness when bainite is being replaced by a mixture of ferrite +pearlite as cooling rate decreases.

The calculation of flow stress curves in steels follows similar procedures as previously described in Ref. [11] for titanium alloys. CAE packages normally provide a range of constitutive equations that describe stress as a function of temperature, strain and strain rate. The user has to first decide which equation to use, as the choice of equation can affect the simulation significantly. He will then be facing the task of assigning proper values to each of the material constants in the constitutive equation. The present approach models materials flow behaviour based on the fundamental deformation mechanisms in operation and is predictive in nature. It automatically determines whether deformation should be dominated either by dislocation glide or by dislocation climb, depending on the

temperature, strain and strain rate regime. The problems associated with picking the right constitutive equation and assigning suitable values to the parameters involved have therefore been completely removed. The flow stress curves at a fixed strain rate of 0.1 s⁻¹ of the austenite phase at various temperatures is shown in Figure 4 as examples. The material flow is dominated by dislocation glide at 600°C and by dislocation climb at 900°C. The deflection

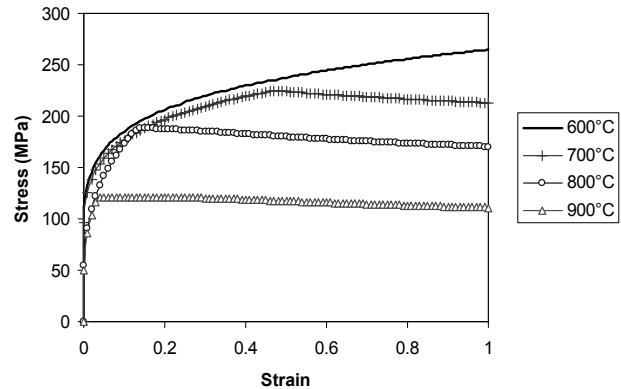


Figure 4. Flow stress curves at various temperatures, strain rate 0.1 s⁻¹.

in the flow stress curves at 700°C and 800°C results from the change in mechanism.

CAE Simulation – Coupled Heat Transfer, Deformation Mechanics and Phase Transformation

Depending on cooling rate and temperature variation, different kinds of phases form and their volume fractions vary at each point of the steel part. In the mean time, temperature variation and cooling rate are influenced by the amount of heat generated according to the kind of phases formed and its volume fraction during phase transformation. Thermal gradient and phase transformation also have a significant effect on the dimensional change and stress distribution. Therefore, coupling of heat transfer, deformation mechanics and phase transformation is essential in hot forming simulation. The mathematical models for the temperature field calculation and stress-strain computations are described below.

Temperature Field. The temperature field is governed by the following equation [12]:

$$\rho c \dot{T} = \frac{\partial}{\partial x_i} \left(k \frac{\partial T}{\partial x_i} \right) + \sigma_{ij} \dot{\epsilon}_{ij}^p + \sum L_{IJ} \dot{\zeta}_{IJ} + \dot{Q} \quad (1)$$

where ρ , c , k and L_{IJ} are density, specific heat, thermal conductivity and latent heat from phase I to phase J , produced by the progressive J^{th} constituent with volume fraction ζ_{IJ} , respectively. \dot{Q} is the heat generated by external heat sources. $\dot{\zeta}_{IJ}$ is the time differentiation of ζ_{IJ} and is termed the transformation rate. The 1st term on the right hand side is from Fourier’s law of heat conduction. The 2nd, 3rd, and 4th terms represent the heat due to plastic deformation (i.e. heat generation by mechanical energy dissipation), the heat absorbed or released during phase transformation, and other heat sources such as eddy current during induction heating.

Deformation Mechanics. The (tensor of) total strain

generated during cooling can be decomposed into various individual strain contributions as follows, given in the form of strain rate for ready adaptation in CAE analysis [13,14]:

$$\dot{\epsilon} = \dot{\epsilon}^e + \dot{\epsilon}^p + \dot{\epsilon}^t + \dot{\epsilon}^{tr} + \dot{\epsilon}^{tp} \quad (2)$$

where ϵ^e , ϵ^p , ϵ^t , ϵ^{tr} , and ϵ^{tp} are the elastic, plastic, thermal, phase transformation, and transformation plasticity strain contributions, respectively. The calculation of ϵ^{tr} and ϵ^{tp} deserves special attention and is described below.

Transformations from austenite to ferrite, pearlite, bainite and martensite give rise to additional strain. This additional strain is one of main factors causing local deformation of the steel part and is proportional to the relative difference in the volume fraction of each phase transformed as follows:

$$\dot{\epsilon}_{ij}^{tr} = \sum \beta_{IJ} \dot{\zeta}_{IJ} \delta_{ij} \quad (3)$$

where β_{IJ} is transformation expansion coefficient and it assumes that all of the phase I transforms to phase J instantaneously, and δ_{ij} represents the Kronecker delta.

Transformation plasticity is a deformation that appears in a transforming material under an applied stress even for the stresses lower than the yield stress of the phases [15]. It will be presented in the directions of the deviatoric stress components. In this study, the transformation plasticity strain in rate term during transformation from phase I to phase J is expressed as [13,15]:

$$\dot{\epsilon}_{ij}^{tp} = 3K_{IJ}(1-\zeta_{IJ})\dot{\zeta}_{IJ}s_{ij} \quad (4)$$

where K_{IJ} and s_{ij} represent the transformation plasticity coefficient and the deviatoric stress, respectively.

Results and Discussion

The CAE simulation package used in this study is DEFORMTM-HT and 2D simulation is performed here. The model contains 552 elements. Yield follows von Mises

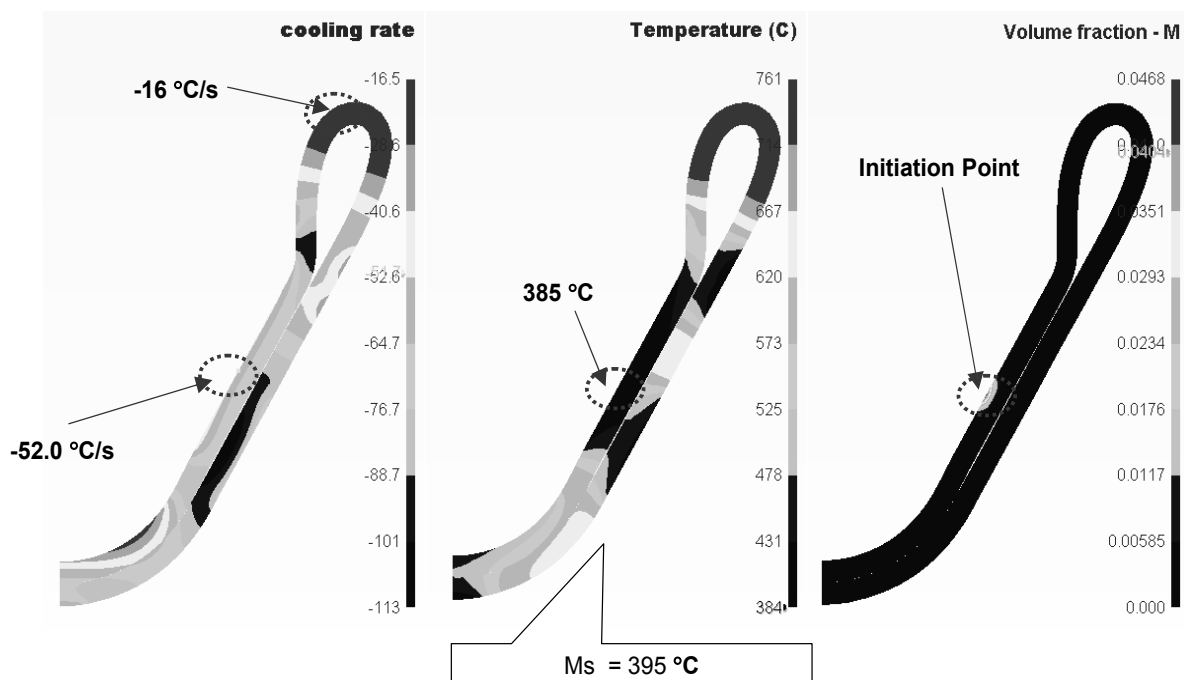


Figure 5. Temperature field, cooling rate distribution and onset of martensite formation (about 1.6 seconds into quenching).

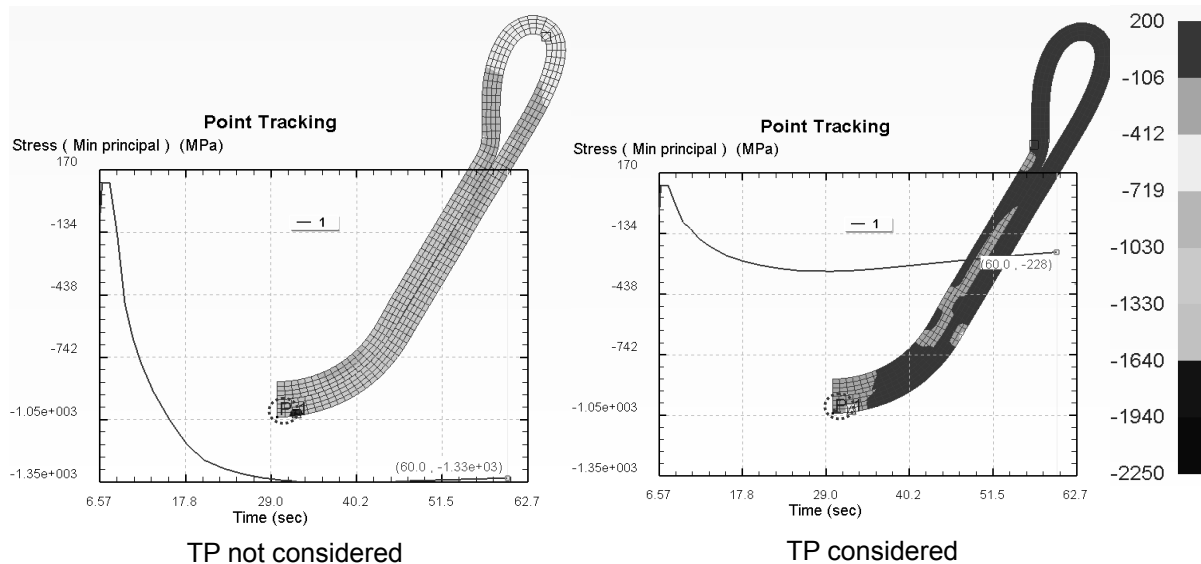


Figure 6. The effect of considering transformation plasticity on the simulated residual stress: point tracking of minimum principal stress evolution during quenching at position P1.

criterion and the material is assumed to harden isotropically. Elasto-plastic quadrilateral element is used to evaluate the stress level accurately and to see the effect of springback after unloading.

The temperature field, cooling rate at each position and volume fraction of martensite formed in the part are shown in **Figure 5**, respectively. It corresponds to 1.6 seconds into quenching, i.e. the onset of martensite formation.

Figure 6 demonstrates the importance of considering transformation plasticity (TP) on simulation. Point tracking of the stress level at position 1 shows that the minimum principal stress after 60 seconds is -228 MPa and -1330 MPa, respectively, with or without TP being considered. If TP effect is not considered, the residual stress in the part would be severely overestimated. The design based on such simulations would be inaccurate.

Figure 7 compares the experimental springback effect with simulation. The die angle is 60°. In experiment, the angle changed from 60° to 61.5° due to springback, whereas that change is from 60° to 62° in simulation. Therefore, the effect of springback is well predicted.

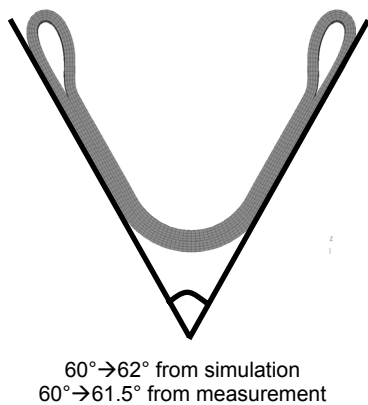


Figure 7. Comparison of experimental and simulated springback effect.

Summary

The development of the JMatPro software has largely provided an answer to the problem of the lack of material data for CAE simulation. It is now able to calculate many physical and mechanical properties when the processing details is known for a given alloy chemistry.

The reliability of CAE simulation also relies on a proper description of all the physical phenomena involved in the processing and a proper consideration of the interactions among them. As demonstrated in this study, neglecting the strain contribution due to transformation plasticity leads to severely overestimated residual stress.

References

- [1] T. Altan: Stamping Journal, Dec. 2006, 40-41.
- [2] T. Altan: Stamping Journal, Jan. 2007, 14-15.
- [3] <http://www.sentsoftware.co.uk/downloads/articles-and-papers.aspx>: A collection of JMatPro-related papers, Sente Software Ltd., 2009.
- [4] Z. Guo, N. Saunders, A.P. Miodownik, J.P. Schillé: Mater. Sci. Eng. A, 499 (2009) 7-13.
- [5] N. Saunders, Z. Guo, X. Li, A.P. Miodownik, J.P. Schillé: JOM, 55 (No.12) (2003) 60-65.
- [6] Z. Guo, N. Saunders, A.P. Miodownik, J.P. Schillé: International Journal of Microstructure and Materials Properties, 4 (2009) 187-195.
- [7] N. Saunders, Z. Guo, X. Li, A.P. Miodownik, J.P. Schillé: The calculation of TTT and CCT diagrams for general steels, Internal report, Sente Software Ltd., 2004.
- [8] Z. Guo, N. Saunders, A.P. Miodownik, J.P. Schillé: Mater. Sci. Eng. A, 413-414 (2005) 465-469.
- [9] Z. Guo, N. Saunders, A.P. Miodownik, J.P. Schillé: The 2nd International Conference on Heat Treatment and Surface Engineering in Automotive Applications, 20-22 June, 2005, Riva del Garda, Italy.
- [10] Z. Guo, N. Saunders, J.P. Schillé: Netsu Shori, 49 (2009), Special Issue vol.2, 753-756.
- [11] Z. Guo, N. Saunders, J.P. Schillé, A.P. Miodownik: MRS International Materials Research Conference, 9-12 June, 2008, Chongqing, China.
- [12] K. Arimoto, D. Lambert, G. Li, A. Arvind, W.T. Wu: SFTC Paper #347, Scientific Forming Technologies Corporation.
- [13] K. Arimoto, H. Kim, M. Narazaki, D. Lambert, W.T. Wu: SFTC Paper #370, Scientific Forming Technologies Corporation.
- [14] S.H. Kang, Y.T. Im: Journal of Materials Processing Technology, 192-193 (2007) 381-390
- [15] S. Denis, E. Gautier, A. Simon, G. Beck: Mater. Sci. Technol., 1 (1985) 805-814.